CLM-R 99

United Kingdom Atomic Energy Authority

RESEARCH GROUP

Report

COLLISIONLESS INTERACTIONS IN INTERSTREAMING PLASMA JETS

P. F. LITTLE
B. E. AVIS
R. B. TURNER

Culham Laboratory
Abingdon Berkshire
1969

Available from H. M. Stationery Office
THREE SHILLINGS AND THREEPENCE

C.18

U.D.C.
533.922

COLLISIONLESS INTERACTIONS IN INTERSTREAMING PLASMA JETS

by

P.F. LITTLE
B.E. AVIS
R.B. TURNER

A B S T R A C T

The potential fluctuations detected by an external probe when two collision-free plasma jets stream through each other in a magnetic field are described. The noise spectrum is enhanced in a frequency range where ions of one plasma are expected to generate noise by their interaction with the common electron cloud. This is the first experimental evidence for the existence of the ion-electron instability in interstreaming plasmas.

The noise spectrum of a single plasma jet shows evidence of an instability driven by the perpendicular velocity of the ions which has been observed previously.

U.K.A.E.A. Research Group,
Culham Laboratory,
Abingdon,
Berks.

April, 1969 C/18 (MEJ)

C O N T E N T S

1. INTRODUCTION

This paper reports some experimental measurements of the potential fluctuations detected by a small external electrode when two plasma jets of low density stream through each other in a uniform guiding magnetic field. The plasmas are created by coaxial rail plasma guns. Previous studies (LITTLE and AVIS, 1966a) have shown that a fast plasma jet containing only H^+ ions and electrons is emitted from a point source near the tip of the inner gun electrode in a very short burst. In the present work we investigate the ion energy range between 5 keV and 40 keV in plasmas whose density is around 10^{11} cm^{-3}.

Any interactions observed must be collision-free phenomena, for the mean free path is greater than 10^4 km for ion-ion collisions and greater than 10^2 km for electron-electron collisions. Earlier measurements by MARSHALL (1958), PARKER (1958) and NEXSEN et al. (1960), in which the diamagnetic signals due to similar plasma jets were measured, showed no enhancement due to interactions when the jets mixed. Denser, slower plasmas following the fast burst produced larger diamagnetic signals as binary collisions scattered the plasma. Collisionless interactions have been seen with dense plasma jets ($\sim 10^{15}$ ions/cm^3) in which magnetic fields exist (ALLEN and COX, 1963). The magnetic pressure is increased when two such jets meet, and the plasmas are deflected from their original paths. BABYKIN et al. (1962, 1964 and references therein) used plasma jets in which the ions had temperatures near 5 eV and directed energies E_i of approximately 100 eV. They found strong interactions when the electron temperature was high ($T_e > E_i$), though the conditions under which

the ion directed energy $1/2\ m_i u_i^2 = E_i$ was randomised seemed to be different in different experiments. When the electrons were cold ($T_e < E_i$) no interaction was seen.

In our experiments $T_e < E_i$, so that interactions of the type considered by Babykin cannot appear. Randomisation of the ion directed energy is not expected. We look for the weaker interaction that should appear due to ion-electron interstreaming according to STRINGER'S theory (1964). Electrostatic instabilities in the plasma are detected by the potential fluctuations induced in a small external disc electrode. The results are compared with theoretical predictions. Some preliminary measurements have been published earlier (LITTLE and AVIS, 1966b).

2. APPARATUS

Fig.1 shows the equipment. Two similar guns constructed of oxygen-free high conductivity copper was used. In each the outer diameter of the annular gap between the electrodes is 7.5 cm, and the inner diameter 5.0 cm: the inner electrode has a rounded tip and is 16 cm shorter than the outer electrode. The gas valve, which has a PTFE seating, lies within the inner electrode, the plenum chamber being 5.5 cm from the tip. This gas valve is opened for a short time by a current pulse through a small water-cooled coil near a conducting plate carried on the valve stem at the back of the gun. Hydrogen is admitted from the plenum chamber through a circle of 12 holes 0.35 cm in diameter in the inner electrode to the annular gap region. Three firing pins trigger the discharge at the gas entry-point. A current I of about 80 kA peak flows in each gun when two 1 μF

capacitors charged to 20 kV are discharged through it using triggered spark gaps. The plasmas produced have been studied by ASHBY (1964), ASHBY and AVIS, (1966), and by LITTLE and AVIS, (1966a).

The guns face each other at either end of a solenoid 2 m long in which a pulsed guide field up to 4 kG can be created. The pulse length is about 1 msec, so that the magnetic field does not penetrate the gun. In the operating mode used here a discontinuity in $\dot{I}$ marks the time at which all the fast plasma is ejected simultaneously from the gun. Four diamagnetic loops are used to find the plasma velocity, knowing the time of ejection.

At the midpoint a copper disc 1 cm in diameter acts as a capacitatively coupled probe. Microwave coaxial cable connects it to a five-way resistive power divider and so to four filters set to cover different frequency bands.

For a source in the plasma the approximate equivalent circuit of the detector is as shown inset in Fig.1. C_1 is the capacity between plasma and probe, while L and C are determined by the probe dimensions and R by the cable impedance. Direct measurement of the impedance of the probe shows a series resonance of L and C i.e. zero impedance at about 2.3 GHz, with $L \approx 2$ nH and $C \approx 2$ pF. Thus with a 50 Ω cable the detector response is expected to fall off above 2 GHz approx. After detection the RF signal amplitudes are displayed on oscilloscopes, together with the $\dot{I}$ signals and the diamagnetic loop outputs.

3. EXPERIMENTAL PROCEDURE

Because the guns do not behave reproducibly many shots are photographed and averaged to obtain mean values. For a given set of

filters and given magnetic guide field normally 15 shots with both guns firing together are taken, then 10 shots of each gun separately and finally another 15 shots of both together. Any shots in which either gun fails to show a discontinuity in $\dot{I}$, or where the diamagnetic loop signals show unusual velocity distributions are rejected. The remaining 'normal' shots are used to find the average power received by the probe when both guns or either gun are fired. The number of shots used to find these averages is between 9 and 50 for individual guns except for four cases in which 5 shots only were taken, and between 5 and 31 for both guns firing together. This wide variation in the number of useful shots is a measure of the irreproducibility of the guns.

This procedure is repeated for different filters and magnetic fields until a band from 50 MHz to 2 GHz has been covered at fields of 500 G, 1 kG, 2 kG and 4 kG. Let the power received by the probe over a frequency range f_a to f_b be P_a, and put $f = 0.5 (f_a + f_b)$. The mean power received in a frequency band $\Delta f = 0.1\ f$ centred on f is

$$P = 0.1\ f\ P_a/(f_b - f_a).$$

The experimental results are presented in terms of P. Let the power received be P_1 when Gun 1 fires alone, P_2 when Gun 2 fires alone and P_s when both guns are fired simultaneously. In practice of course the term 'simultaneous' must be defined 'coincident within $\pm\ \tau$ secs' where τ is very small. For the results presented $\tau = 0.05$ μsec. This allows a difference in velocity of ± 11% for the highest energy ions and ± 4% for the lowest energy ions studied.

If there were no interaction at all between the plasma jets then $P_s = P_1 + P_2$. We show in the next section the computed results

for P_s and $(P_1 + P_2)$ for various conditions, giving the mean values and the standard errors. For the sum of the signals when the guns are fired individually we write $P_I = P_1 + P_2$.

With the small value of τ allowed the fastest plasma from Gun 1 cannot disturb the initial firing of the opposite gun. It has been found that at the instant of firing a short burst of high-energy electrons is sometimes ejected from these guns, but this is over before the plasma emerges from the gun. Any noise generated in a plasma by electrons from the other gun would die away in a few plasma periods ($\lesssim 10^{-9}$ sec) and would not contribute to the measurements here. This was shown in our earlier work, when noise enhancement at high frequencies was observed at the time of plasma ejection (LITTLE and AVIS, 1966a).

4. EXPERIMENTAL RESULTS

In Figs. 2 to 5 the values of P_s are shown, together with the standard errors in the observations, for ions of energies 5,10,20 and 40 keV in magnetic fields of 0.4, 1.2 and 4 kG. The frequency ranges of the filters used are shown in Fig.2.

In each figure the values of P_I are shown also. Error bars are not given for P_I, to avoid confusion in the figures; the errors are in general smaller than the errors in P_s.

It is seen that a large peak at about 80 MHz appears in nearly all these noise spectra. No other common feature is obvious, but at low energies and low magnetic field the general noise level falls off.

In Figs. 6 to 9 the ratio of P_s/P_I as a function of frequency is shown for the higher frequencies, excluding the region around

80 MHz. Error bars are given for results at 2 kG for the four energies. The upper limit of the error estimates is obtained by taking the largest value of P_s and the smallest value of P_I within the standard errors of each, and the lower limit by using the opposite extremes. The large errors, and the large scatter in the points, emphasise that the guns produce very variable plasmas. Nevertheless, the ratio of P_s/P_I is significantly greater than unity at the higher energies over a range of frequencies from 200-2000 MHz.

5. THE NOISE GENERATED IN A SINGLE PLASMA JET

From previous measurements on these coaxial guns we know that they act essentially as point sources of energetic ions accompanied by neutralising electrons (ASHBY and AVIS, 1963). The maximum ion energy observed in 65 keV (LITTLE and AVIS, 1966) and the electron temperature is approximately 50-100 eV. The ion density varies with energy, being largest at about 5 keV and less for lower energy ions. Impurity ions have energies less than 1 keV, and do not contribute to the interactions studied here.

The mean densities n as a function of ion velocity v_z observed in our previous work depended on the delay between the entry of the neutral gas and the start of the discharge, initiated by a voltage pulse applied to the trigger electrodes. In these experiments reported here the trigger delays were set to give the clearest discontinuity in I, thus yielding the highest plasma densities. The values for $B_z = 2$ kG are given in Table 1. These values are used for all calculations.

TABLE 1

DENSITY OF PLASMAS FOR DIFFERENT ENERGIES

Ion Energy E_z (keV)	Ion Velocity v_z (cm sec^{-1})	Mean density n (cm^{-3})
5	1×10^8	3×10^{11}
10	1.4×10^8	1.5×10^{11}
20	2×10^8	9×10^{10}
40	2.8×10^8	4.5×10^{10}
65	3.7×10^8	0

These densities will be approximately correct for fields of 1 and 4 kG also, but they overestimate the density at 0.4 kG. The results for the lowest magnetic field are included to show their general similarity to the remainder.

The fast hydrogen ions possess perpendicular energies of the order of 500 eV, giving them a large Larmor radius a_i (about 4 cm in a magnetic field of 1 kG). In the outer regions of the plasma column then an ion diamagnetic current dominates, and an instability of very fast growth rate can exist (ASHBY and PATON, 1967). A solution has been obtained only for the case where $k_z/k_y \approx (m_e/m_i)^{\frac{1}{2}}$, using a slab model: a characteristic frequency ω_o given by

$$\frac{1}{\omega_o^2} = \frac{1}{\omega_{pi}^2} + \frac{1}{\omega_{ci}\,\omega_{ce}}$$

appears, dependent on the ion plasma frequency ω_{pi} and on the cyclotron frequencies ω_{ci}, ω_{ce}. It is assumed that a beam of ions flows perpendicular to B_z, representing ion orbits with large Larmor radii.

For this special case the frequency of the fastest growing instability is $\omega_m = 0.87\ \omega_o$ and the maximum growth rate is $\gamma_m = 0.5\ \omega_o$. The wavenumber corresponding to ω_m is $k_m = 1.7/v$, where $v_\perp$ is the ion velocity perpendicular to B_z. It is likely that these values represent the fastest-growing waves in the spectrum (HAAS, 1969, private communication); at any rate the instability they describe is so fast-growing that it will contribute strongly to the noise in the plasma. There is however one limitation, for if $T_i < 3\ T_e$ the assumptions used become invalid.

In the outer regions of our plasma jets $T_{i_\perp} \leqslant 500$ eV. The effect of the instability then should be to heat the plasma electrons at least until $T_e \sim 0.3\ T_{i_\perp} \sim 100$ eV, where the assumptions fail. This is the model suggested by ASHBY and PATON to explain the loss of transverse ion energy observed as fast plasma jets move along a magnetic guide field (see ATKINSON and PHILIPS, 1967 and references therein). Thermal conduction in the electron gas along field lines to the wall of the vacuum vessel cools the electrons, so that the instability is expected to persist at a level that will balance the loss of energy to the walls.

At the edge of the plasma the ion density is taken to be half the mean values shown in Table 1; for ions of various energies the instability parameters are given in Table 2, with $f_m = \omega_m/2\pi\ \text{sec}^{-1}$.

The influence of the magnetic field on f_m is always less than 5%. The final column gives the Doppler shift expected due to the plasma motion. This is always small, though a range of k_z is to be expected in practice and the Doppler shifts might become comparable with f_m.

TABLE 2

INSTABILITY DUE TO TRANSVERSE ION STREAMS

Ion Energy E_{iz}(keV)	Ion Velocity V_{iz}(cm sec^{-1})	Plasma density $n(cm^{-3})$	f_m MHz	γ_m sec^{-1}	k_y cm^{-1}	k_z cm^{-1}	$k_z v_z$ MHz
5	10^8	1.5×10^{11}	60	2.2×10^8	7.2	.17	17
10	1.4×10^8	7.5×10^{10}	42	1.5×10^8	3.6	.085	12
20	2×10^8	4.5×10^{10}	33	1.2×10^8	2.0	.048	10
40	2.8×10^8	2.2×10^{10}	23	$9 \quad 10^7$	1.0	.024	7

In the experiment the probe defects local fluctuations in potential due directly to these unstable waves because the wavelengths involved are long ($\lambda_y \approx$ 1-5 cm, and $\lambda_z \gg \lambda_y$). In addition, the instabilities cause fluctuations in the particle loss rate from the plasma which are observed because the local potential of the plasma is affected.

Noise appears at frequencies near 80 MHz and at harmonics of this frequency in the P_I spectra shown in Figs.2 to 5. This can be attributed to the instability just described. In Fig.2, at B_z = 0.4 kG and $E_z \leq$ 10 keV, no peaks appear: this is because the ions with high transverse energy are lost after one cyclotron orbit ($a_i > R$, the tube radius). Thus no transverse ion beam exists to drive the instability after $\tau > 2\pi/\omega_{ci}$ i.e. τ = 0.64 μsec, less than the time for 10 keV ions to reach the probe.

6. THEORY OF NOISE IN INTERSTREAMING PLASMAS

(a) Electrostatic instabilities in zero magnetic field

We shall not discuss the frequency range below 200 MHz, where P_s is approximately the same as P_I, i.e. merely a superposition of two independent spectra. Effects due to interstreaming are masked by the violent instability in each isolated jet discussed in Section 5 above.

Above 200 MHz we use STRINGER'S theory (1964). In the plasmas here $T_e \approx$ 50-100 eV, and we take the densities from Table 1. An estimate for an upper limit of the ion temperature $T_{i_{\parallel}}$ is found from observations of ASHBY and AVIS (1963). They measured variations of approximately $\pm 10^{-8}$ sec in the time of emission of the plasma jets, so that at a given position at any instant the transit time of the ions from one gun can vary by times of this order at most. This defines a maximum velocity of random motion for the ions along the magnetic field corresponding to $T_{i_{\parallel}} < 14$ eV at the midpoint.

Let each gun be s cm from the midpoint of the field coils, where the probe is placed: set 2L as the length of the coil assembly, and consider the plasma interaction at a distance x from the midpoint t sec after the guns have fired. Let the nearest gun be Gun 1 giving ions of energy v_1 over a time interval τ_1.

Then $t = (s-x)/v_1$ and the range of ion energies present from Gun 1 is δv_1 given by

$$\delta v_1/v_1 = \tau_1/t = \tau_1 v/(s-x).$$

Hence the ion 'temperature' to be associated with the plasma from Gun 1 gives a velocity of random motion

$$c_{i1} = \tau_1 v_1^2/(s-x) \qquad \ldots (1)$$

and for the other plasma

$$c_{i2} = \tau_2 \, v_2^2/(s+x) \qquad \ldots (2)$$

where

$$v_2 = v_1(s+x)/(s-x).$$

We assume that the electrons and ions of each plasma have a Maxwellian distribution, the electron temperature being constant with x and the ion temperature varying as described by equations(1) and (2).

The densities of each plasma are defined from Table 1 if we ignore the variation of density with distance. This is about $\pm$ 20% which is $\pm$ 10% in the plasma frequency: such a small change is negligible here.

The electrostatic interaction between two infinite Maxwellian plasmas has been treated by several authors; Stringer gives an approximate solution for the case where T_{e1}, T_{e2}, T_{i1} and T_{i2} can all take different values and where v_1 can differ from v_2. He finds that for a wavenumber k a frequency ω of the wave that will propagate with a growth rate Υ is given by

$$k^2 = -\sum_j \frac{1}{\lambda_j^2} D\left[\frac{(\omega_1/k) - v_j}{\sqrt{2}\, c_j}\right] \qquad \ldots (3)$$

$$\frac{\Upsilon}{k} = \frac{\sqrt{\pi}}{2} \frac{\sum_j \frac{1}{\lambda_j^2 c_j}\left[(\omega_1/k) - v_j\right] \exp\left\{-\left[(\omega_1/k) - v_j\right]^2/2c_j^2\right\}}{\sum_j \frac{1}{\lambda_j^2 c_j} E\left[\frac{(\omega_1/k) - v_j}{\sqrt{2}\, c_j}\right]} \qquad \ldots (4)$$

where j groups of charged particles (ions or electrons) are present having drift velocities v_j and densities n_j. In (3) and (4):-

$$D(x) = 1-2x \exp(-x^2) \int_0^x \exp(y^2)\, dy$$

$$E(x) = x + (1-2x^2) \exp(-x^2) \int_0^x \exp(y^2)\, dy$$

$$c_j^2 = kT_j/m_j$$

$$\lambda_j = c_j/\Omega_j$$

$$\Omega_j^2 = 4\pi n_j e_j^2/m_j$$

In our experiment $0{\cdot}1 < v_j/c_e < 1$, so that neither electron-electron interstreaming nor ion-ion interstreaming can create growing waves (see Fig.3 of Stringer's paper). This leaves only the possibility of an interaction between the fast ions of one plasma with the common electron cloud. If $T_e/T_i > 4$ approximately then ion-acoustic waves in the frame of reference of the moving ions are unstable: the weighted (ion + electron) energy distribution shows a sufficient positive gradient to allow this. In our experiment values of $T_{i_{\parallel}} \leqslant 14$ eV and $T_e \sim 100$ eV are expected, so that the ion-electron instability should appear.

(b) Effects due to currents and the magnetic field

(i) Current-driven instabilities

Our previous experiments (1966a) have shown that with a conducting obstacle in the drift tube the noise enhancement at high frequencies vanishes. Thus when axial currents are allowed but interstreaming is forbidden the instability does not occur. This demonstrates that no significant axial currents are following here, though axial currents are important in some turbulent heating experiments (HAMBERGER and FRIEDMAN, 1968).

(ii) Hydromagnetic instabilities

If the directed energy of the plasma is sufficiently high, unstable Afven waves are possible (LOMINADZE and STEPANOV, 1965). Writing

$$\beta_{\parallel} = \frac{1}{2} m n v_z^2/(B^2/8\pi)$$

instabilities are predicted if $\beta_{\parallel} > 0.7$. For our lowest magnetic field (0.4 kG) $\beta_{\parallel} \lesssim 0.7$, so all the plasmas should be stable hydromagnetically.

Although the probe used here detects potential fluctuations, we would expect to observe any hydromagnetic instabilities present because the associated plasma density fluctuations should produce some changes in the electric field pattern at the probe. It is therefore important that this class of instabilities can be dismissed.

(iii) Cyclotron resonances

BALDWIN and ROWLANDS (1966) have shown that the effect of a magnetic field on the collisionless damping or growth of electrostatic waves can be neglected if the cyclotron frequency ω_{ci} is small compared to the imaginary part of the wave frequency i.e., we may neglect all ion cyclotron instabilities if $|\gamma|/\omega_{ci} > 1$. The values of γ calculated in the next Section lie in the range $1\text{–}4.10^7$ sec^{-1} usually, compared to a maximum for $\omega_{ci} = 4.10^7$ rad sec^{-1} in a field of 4 kG. Thus $\gamma/\omega_{ci} \approx 1$, a region where the cyclotron resonance begins to operate. Its effect is to give bands of noise at harmonics of ω_{ci}, and to introduce waves propagating at an angle to the field (CRAWFORD, 1965). Obviously the cyclotron harmonics are much too closely spaced to be detected by our broad filter bands ($f_{ci} \lesssim 7$ MHz),

and the existence of a small but finite $k_\perp$ would not affect the detection of the perturbations by our external probe. If $\gamma > \omega_{ci}$, the harmonic bands merge together and the summation over all harmonics leads to the growth or damping deduced for zero magnetic field (see BALDWIN and ROWLANDS, 1966). We are approaching this state. We conclude that ion cyclotron resonance effects are present, but probably not significant and certainly not detectable.

The electron cyclotron frequency is so high that instabilities near f_{ce} are usually outside the range of interest here. At 0.4 kG $f_{ce} \sim 1200$ MHz, which is in the observed range: however no growth is observed at this magnetic field for frequencies near f_{ce}. We can then neglect this type of interaction always.

7. COMPARISON OF THEORY AND EXPERIMENT

Since no other instability except that due to ion-electron interstreaming is important any enhanced noise is evidence for this instability. We can however also calculate the range of unstable frequencies expected from theory and compare this with experiment.

Since the fastest growth rate appears for the densest plasmas, we should use the axial density in the calculation; Table 1 gives the mean density, and we take twice the values shown there. We proceed by dividing the interaction region into segments 10 cm in length and calculating the parameters for each section from equations (1) and (2) for assumed pairs of values of T_e and T_{io}, T_{io} being the value of $T_{i_\parallel}$ at the midpoint. As slow ions of one plasma approach the probe they will interact with faster ions of the other plasma,

and equations (3) and (4) are solved to obtain $\Upsilon(\omega)$ for the unstable frequency band for each 10 cm segment. The total growth is obtained by summing the values of $\Upsilon(\omega)$ so found, and multiplying by two to obtain the theoretical power gain P_s/P_I.

Four pairs of values of T_e and T_{io} have been selected for these computations, carried out on the Culham KDF 9 machine.

TABLE 3

VALUES OF T_e AND T_i USED IN THE THEORY

Curve	T_e	T_i
A	70	10
B	100	10
C	70	7
D	100	7

The theoretical curves should lie above the measured ratios of P_s/P_I (see Figs. 5 to 8) for several reasons. First, the ions are moving in Larmor orbits of significant radius, so that they sample plasmas of varying density, always less than the density on the axis. This has the effect of reducing Υ, so the ratio P_s/P_I calculated is an upper limit. Second, the measured values of $P_I(\omega)$ include perturbations of all k values, so that the measured ratios P_s/P_I are less than the true growth rates in the experiment. They represent a lower limit to the values actually existing. Finally, the other oscillations prsent may interact with the waves excited as the plasmas mix to give a non-linear damping effect which again reduces P_s/P_I.

Comparing the curves with the experimental points, we see that for 5 keV ions (Fig.6) curve A predicts no instability at all, and curve B only small growth over a narrow frequency range. A small change in T_i from 10 eV to 7 eV with T_e = 70 eV gives curve C, which lies above the observed points. No growth is observed above 800 MHz here, in accord with theoretical expections.

At high energies the observed upper frequency limit for growth becomes higher, and the predicted curves move in the same way by about the right amount. The theoretical growth rates are higher than those observed for 10 keV and 20 keV ions, as expected, though for the 40 keV ions, curve C is almost a best fit to the points. By assuming T_e = 100 eV to obtain curve D the theoretical curve is again brought above most of the experimental values.

The closer agreement between theory and observation for the 40 keV ions is understandable. The high energy plasmas interact only over a short distance near the midpoint, and the time of interaction is small compared to their orbital period. Hence the ions on the axis remain close to it, and the experimental growth rate should approach the calculated one. In addition, as the frequencies involved are high, competing noise sources are generally of less significance so that the observed ratios of P_S/P_I ought to be closest to the true growth rates in the plasma and non-linear damping of least importance for these high energy ions.

The theory of Stringer then predicts an electrostatic instability in the frequency range where an instability is observed. The growth rate is consistent with observation, although it cannot be critically tested here. The experiments define only the unstable frequencies:

we have no knowledge of the unstable wavenumbers. Theory predicts short wavelengths for the instability ($\lambda_z \approx 0.3$ cm) so the probe must be detecting fluctuations in plasma potential due to variations in the particle loss rate near the probe.

8. CONCLUSION

Potential fluctuations detected by an external probe show that in opposed plasma jets ion-electron interstreaming instabilities appear. With the plasma parameters used no collisions occur and no other instabilities can contribute significantly to the enhanced fluctuations, though ion cyclotron resonance phenomena may modify the instability a little. Lower-frequency noise in single plasma jets is consistent with another instability due to the ion diamagnetic current in the plasma.

9. ACKNOWLEDGEMENTS

We wish to thank T.E. Stringer for discussions on the theoretical aspects of this work.

10. REFERENCES

ALLEN, T.K. and COX, A.J. (1963) Bull. Am. Phys. Soc. 8, 441.

ASHBY, D.E.T.F. (1964) Proc. Sixth Int. Conf. Ionization Phenomena, Paris, 1963 4, 665.

ASHBY, D.E.T.F. and AVIS, B.E. (1966) Plasma Phys. 8, 1.

ASHBY, D.E.T.F. and PATON, A. (1967) Plasma Phys. 9, 359.

ATKINSON, D.W. and PHILLIPS, J.A. (1967) Culham Report CLM - R 72.

BABYKIN, M.V., ZAVOISKII, E.K., RUDAKOV, L.I. and SKORYUPIN, V.A. (1962) Zh. Eks. Teor. Phys. 43, 1976: (J.E.T.P. (1963) 16, 1392).

BABYKIN, M.V., GAVRIN, P.P., ZAVOISKII, E.K., RUDAKOV, L.I., SKORYUPIN, V.A. and SCHOLIN, G.V. (1964) Zh. Eks. Teor. Phys. 46, 511: (J.E.T.P. (1964) 19, 349).

BALDWIN, D.E. and ROWLANDS, G. (1966) Phys. Fluids 9, 2444.

CRAWFORD, F.W. (1965) J. Res. NBS 69D, 789.

HAMBERGER, S.M. and FRIEDMAN, M. Phys. Rev. Letters (1968) 21, 674.

LITTLE, P.F. and AVIS, B.E. (1966a) Plasma Physics 8, 11: (1966b) Proc. Seventh Int. Conf. Ionized Gases 2, 420.

LOMINADZE, D.G. and STEPANOV, K.N. (1965) Zh. Tekh. Fiz. 35, 148 (Soviet Physics Tech. Phys. 10, 113).

MARSHALL, J. (1958) Proc. Second U.N. Conf. Geneva 31, 341.

NEXSEN, W.E., CUMMINS, W.F., COENSGEN, F.H. and SHERMAN, A.E. (1960) Phys. Rev. 119, 1457.

PARKER, E.N. (1958) Phys. Rev. 112, 1429.

STRINGER, T.E. (1964) Plasma Physics 6, 267.

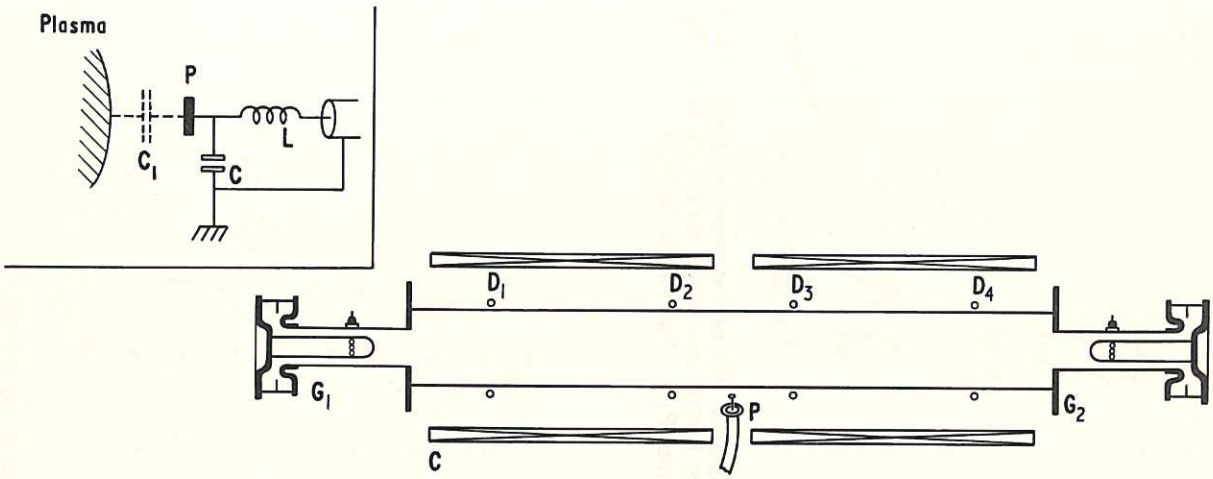

Fig. 1 Apparatus. G_1 and G_2 are identical coaxial plasma guns, D_1 D_2 D_3 and D_4 are diamagnetic loops, P is the capacitative probe used to detect potential fluctuations. Inset: The equivalent circuit of the probe P.

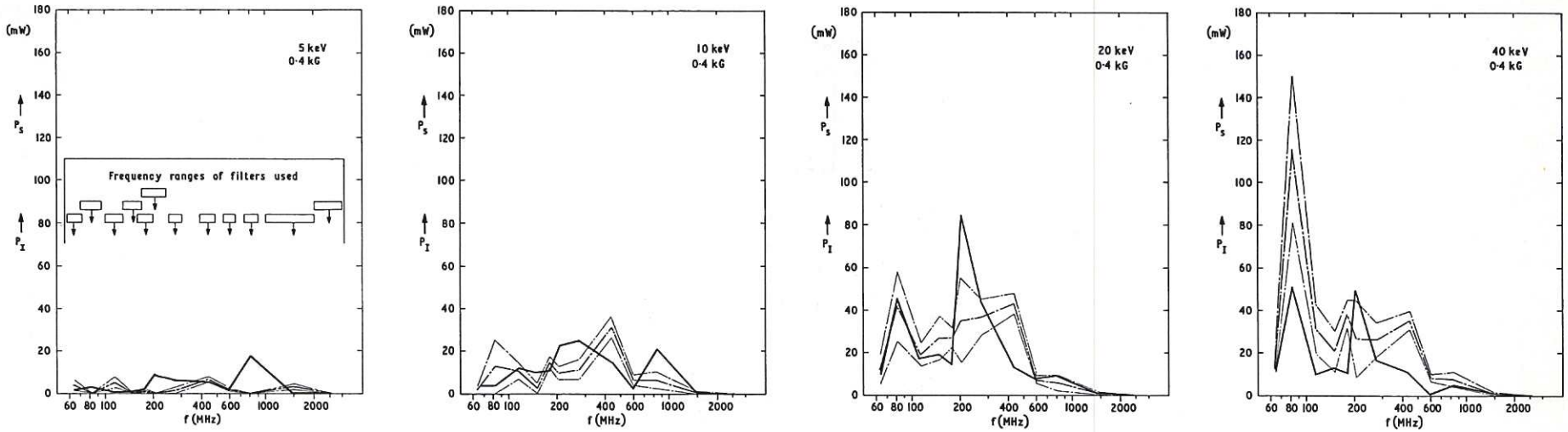

Fig. 2 Mean power received over a frequency band equal to 10% of the mean frequency, using the pass-bands shown. Results for simultaneous firing of both guns, with error limits, are shown by broken lines (P_S): the sum of the output for each gun fired individually is given by the solid line (P_I). The magnetic field B_Z is 0.4 kG

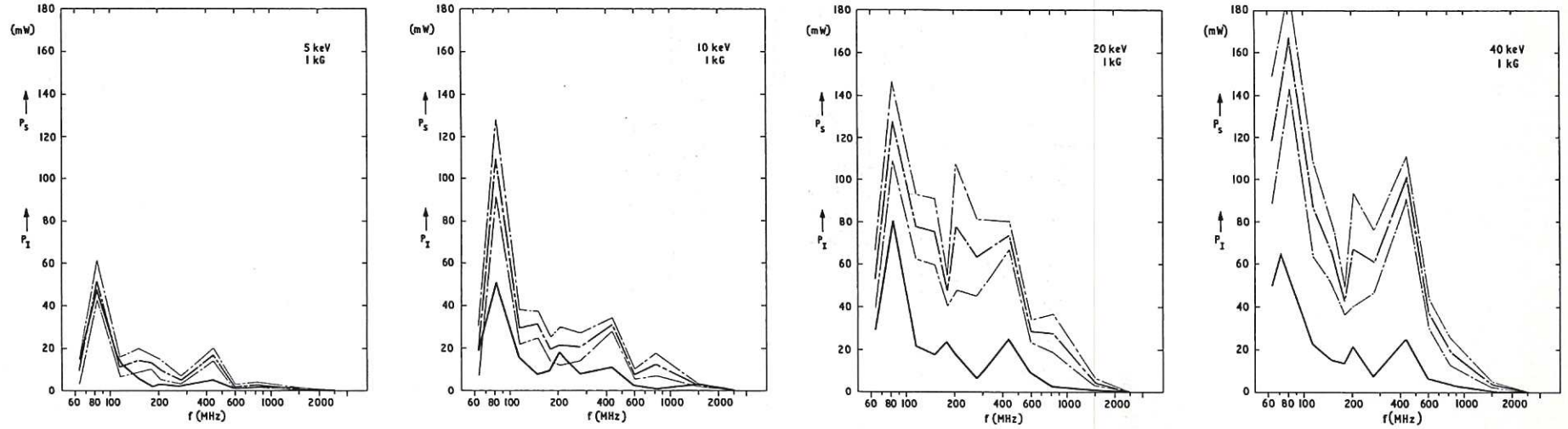

Fig. 3 $B_Z = 1$ kG

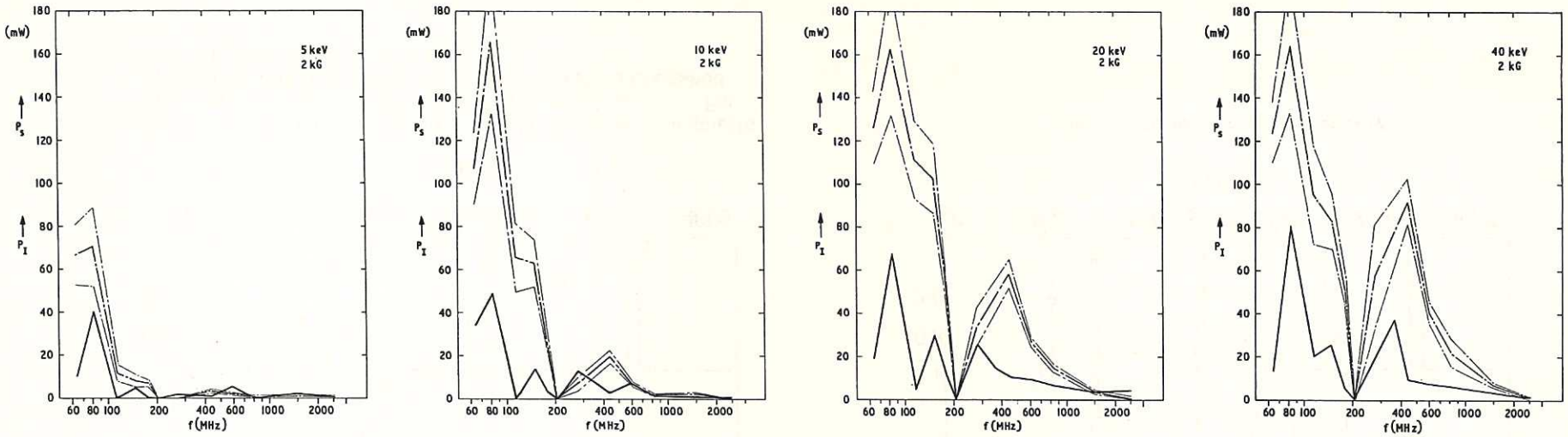

Fig. 4 Mean power received over a frequency band equal to 10% of the mean frequency, using the pass-bands shown. Results for simultaneous firing of both guns, with error limits, are shown by broken lines (P_S): the sum of the output for each gun fired individually is given by the solid line (P_I). The magnetic field B_Z is 2 kG

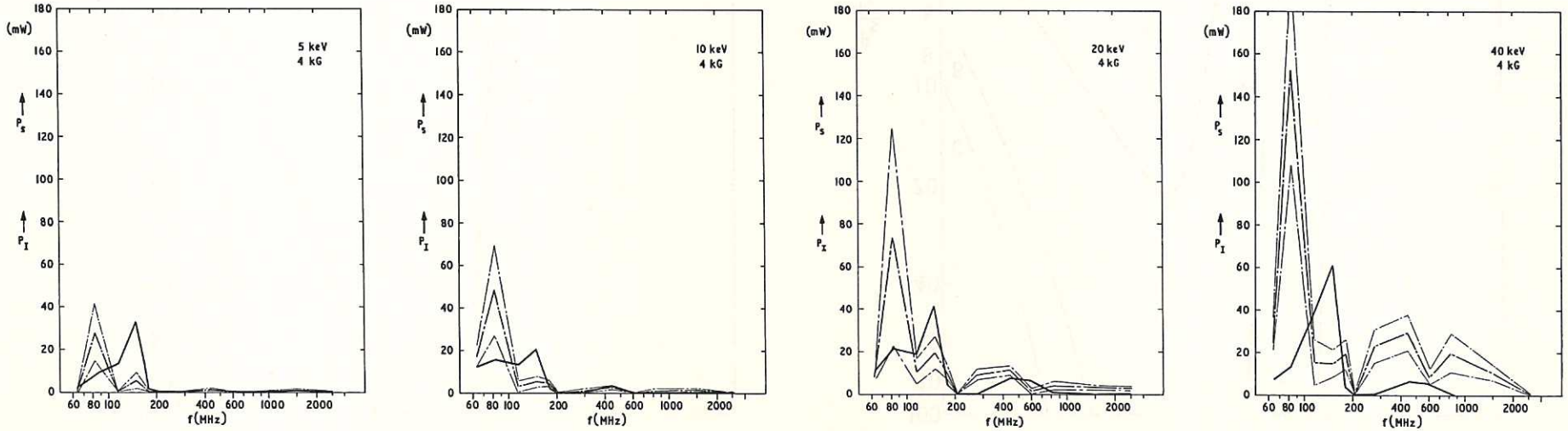

Fig. 5 $B_Z = 4$ kG

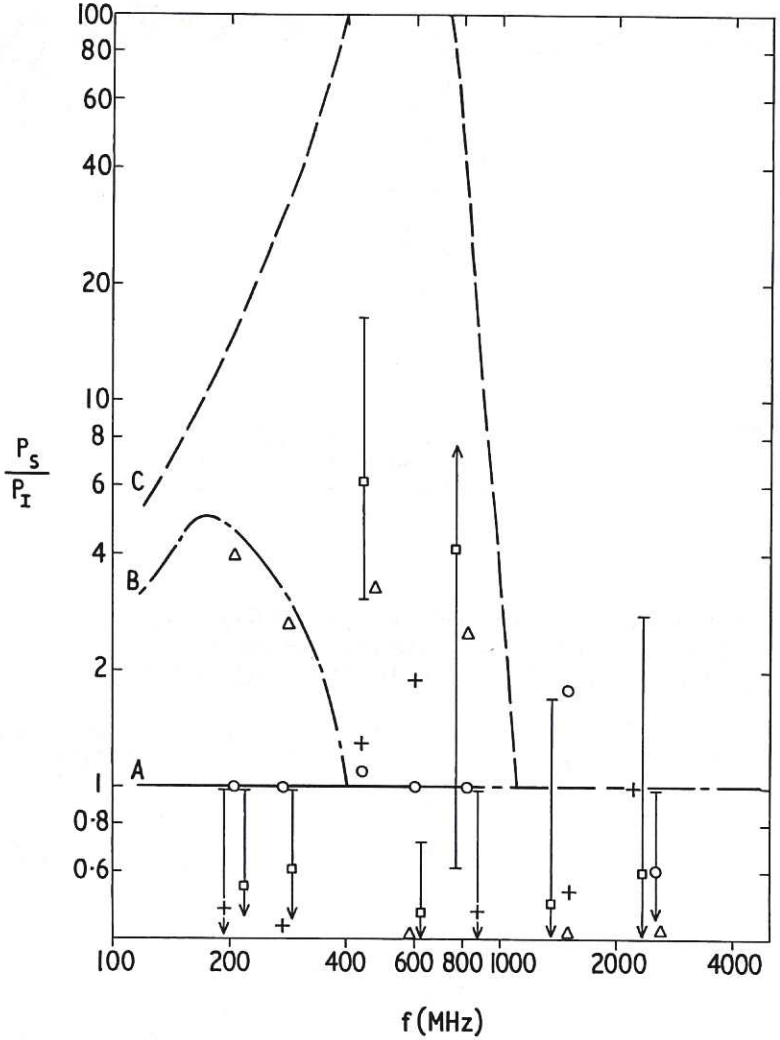

Fig. 6 The ratio P_S / P_I for ions of 5 keV energy in magnetic fields of 0.4 kG (+), 1 kG (Δ), 2 kG (□) and 4 kG (○). For theoretical full-line curve (A), broken line (B) and dashed line (C), refer to Table 3 in text.

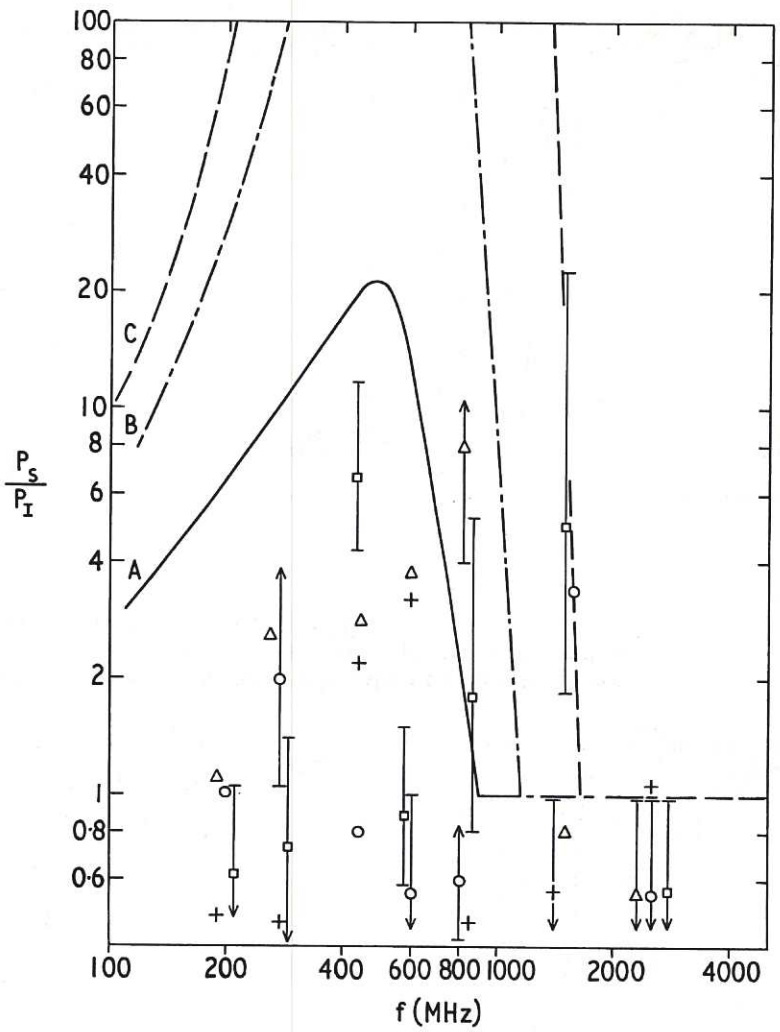

Fig. 7 For ions of 10 keV energy

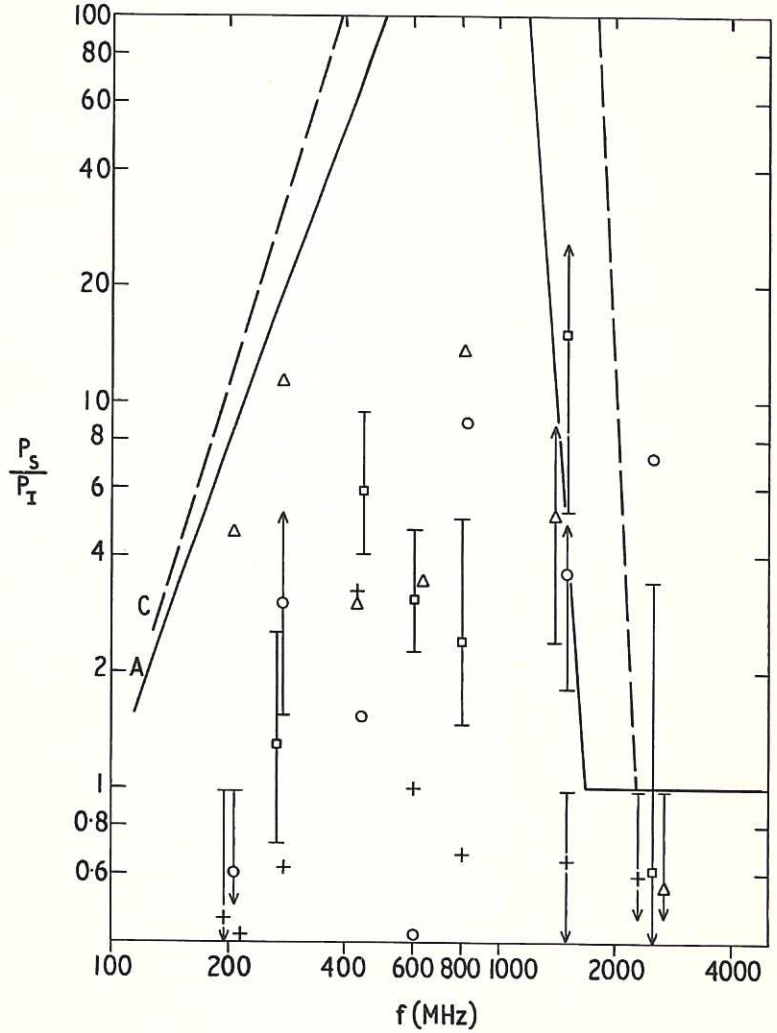

Fig. 8 The ratio P_S / P_I for ions of 20 keV energy in magnetic fields of 0.4 kG (+), 1 kG (Δ), 2 kG (□) and 4 kG (○). For theoretical full-line curve (A), broken line (B) and dashed line (C), refer to Table 3 in text.

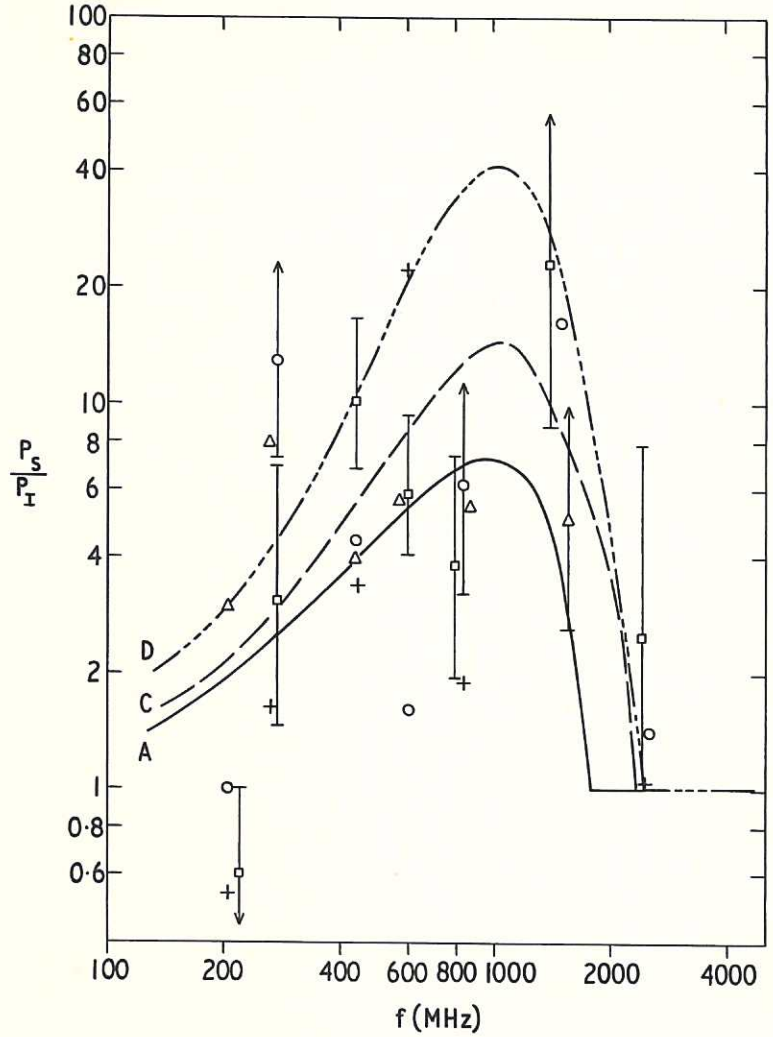

Fig. 9 For ions of 40 keV energy

Available from

HER MAJESTY'S STATIONERY OFFICE

49 High Holborn, London, W.C.1
13a Castle Street, Edinburgh 2
109 St. Mary Street, Cardiff CF1 1JW
Brazennose Street, Manchester M60 8AS
50 Fairfax Street, Bristol BS1 3DE
258 Broad Street, Birmingham 1
7-11 Linenhall Street, Belfast BT2 8AY

or through any bookseller.